Physical principles of the single-C_{60} transistor effect

C. Joachim
CEMES-CNRS, 29 rue J. Marvig, Boîte Postale 4347, 31055 Toulouse Cedex, France

J. K. Gimzewski
IBM Research Division, Zurich Research Laboratory, 8803 Rüschlikon, Switzerland

H. Tang
CEMES-CNRS, 29 rue J. Marvig, Boîte Postale 4347, 31055 Toulouse Cedex, France

(Received 25 June 1998)

Starting with the physics of tunneling transport through a molecule, we describe the principles underlying electrical amplification effects of a C_{60} molecule. We discuss in detail the consequences of intramolecular electronic-level repulsion, an effect induced by compression of the molecule, which leads to an exponential variation of the current for a minute compression of the molecule. This detailed understanding underpins the C_{60} amplifier. Using a planar configuration and an independent electromechanical grid, a transistor effect results from this repulsion effect. [S0163-1829(98)07448-7]

I. INTRODUCTION

An electrical amplifier, which in its present form uses only one C_{60} molecule as its basic element, has been described briefly in Ref. 1 and some of its technological consequences in Ref. 2. We present here details of the basic physics underlying this nanoscale amplifier. This serves as the basis for going beyond these findings to produce a transistor effect, which results from using the same principle and a third, independent electrode.

A schematic diagram of our proposed molecular transistor is shown in Fig. 1. Two point nanocontacts, analogous to the tips used in scanning tunneling microscopy (STM), are positioned in close nanoproximity ($\approx 1-10$ nm) to one side of the molecule. One of the electrodes, the source, is connected to ground and the other (the drain) to the bias voltage V_b via the load. A very small electromechanical actuator (the grid) is prepositioned at a van der Waals distance to the other side of the molecule (Fig. 1). The input signal V_g on the electromechanical element produces (by compression) a change in the intramolecular conformation of the molecule. The transresistance of the source-molecule-drain junction is modified by this compression and, as a consequence, so is the drain-source effective tunnel barrier height ϕ. This was the original transistor effect we proposed based on the fact that ϕ is modulated by a third electrode, the V_g of which is lower than V_b.[2]

In solid-state transistors, electric fields are commonly used to control channel transresistances.[3] At the molecular scale, it is not yet clear how or whether an electric field can play an equivalent role because of the high-field strength required to polarize a molecule significantly. More importantly, the required field strength is incompatible with the structural stability of source and drain nanocontacts. Therefore, to show that a gain can be obtained with a nanoscale device, an electromechanical grid based on an electromechanical device, originally piezoelectric in nature, was used.[1]

In a simple metal-vacuum-metal junction, modulation of the vacuum tunnel barrier was recently proposed by McCord, Dans, and Pease to achieve a transistor effect with a large gain.[4] In vacuum, the spreading of the wave functions outside of the electrodes ensures a through-space electronic coupling between these electrodes, and supports a tunneling current intensity written[5]

$$I_d = I_0(V_b)e^{-2\gamma_0 L}, \tag{1}$$

where γ_0^{-1} is the inverse tunneling damping length through the vacuum ($\gamma_0 \approx 1$ Å^{-1} for noble-metal electrodes[5]). Therefore modulation of this barrier can, in principle, be achieved through actuation by changing either I_0, γ_0, or L using a third electrode.

At small L ($L < 0.5$ nm), the value of γ_0 is small compared to 1 Å^{-1} owing to the collapse of the tunnel barrier.[6] Consequently, no gain can be reasonably expected by modu-

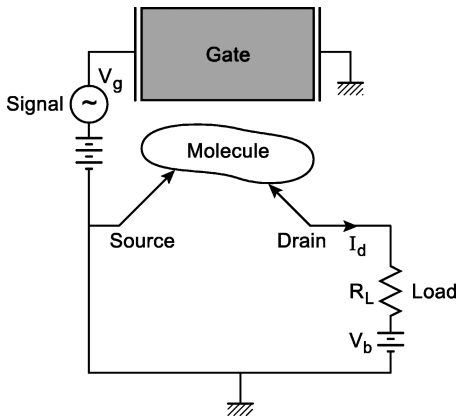

FIG. 1. Schematic of an electromechanical single-molecule transistor. The grid consists of a small piezoelectric crystal compressing the molecule held between the source and drain electrodes. The grid signal V_g is applied over a setup grid voltage necessary to preposition the piezo near the molecule. The output signal is measured across the load R_L, with V_b the bias voltage of the device.

lating L, and even the associated metal-adhesion problems do not allow multiple cycling of the device. Nevertheless, an atomic relay was experimentally realized by Smith using the propensity of metallic tunnel barriers to collapse at small L, thereby opening quantized ballistic channels between the metallic electrodes.[7]

At large L, γ_0 can be maintained at stable values, and a change of L by 1 Å results in a typical increase of one order of magnitude in I_d. Under these circumstances, modulating L by a gate voltage V_g (Ref. 4) produces a transconductance g of the device of

$$g = \frac{dI_d}{dV_g} = -2\gamma_0 I_d \frac{dL(V_g)}{dV_g}. \tag{2}$$

This was estimated to lead to a g/I_d ratio as large as 200 V^{-1}, which is one order of magnitude higher than that of a bipolar transistor.[4] The working current of this device is nevertheless in the nanoampere range and not in the milliampere range as is typical for bipolar devices.

One solution proposed to circumvent this problem is to increase the section of the metallic electrodes.[4] This clearly defeats the ultimate objective of fabricating a nanoscale transistor, and thereby fundamentally represents a bad scaling law. Another solution we pioneered is to introduce some kind of material into the tunneling junction, such as atoms or molecules. As measured experimentally,[8,9] $I_0(V_b)$ at constant V_b in Eq. (1) generally increases in such a situation. Fundamentally, this occurs because the overlap of the metal wave functions in the tunnel barrier is better if the barrier contains atoms. Compared to atoms, molecules are predefined building blocks that are capable of attaining the exact dimensions of a tunnel barrier and can be engineered to possess a large number of internal degrees of freedom. Therefore a molecule can be selected not only for its action on I_0 but also as the active channel for a transistor.

One effect we have recently explored experimentally is the near doubling of the apparent value of ϕ by tunneling through a compressed C_{60} molecule.[9] A voltage amplification effect results by modulating L in the range of optimized compression of the C_{60} cage.[1] This effect is discussed here in a more detailed manner in terms of an intramolecular level-repulsion phenomenon. Furthermore, we extend this concept to improve the effect by keeping L and V_b constant and compressing the cage directly using a third electrode.[2] As will be demonstrated, a level-repulsion phenomenon also takes place in this case and is used to control I_0 independently of the source and drain electrodes as proposed in Fig. 1. We also show that the transistor effect is not only specific to C_{60} but to molecules in general with degenerated highest-occupied and lowest-unoccupied molecular orbital (HOMO-LUMO) manifolds.

Conceptionally the action of a single molecule as a transistor requires a deeper insight into the nature of the current flowing from the drain to the source via the molecule. This is provided in Sec. II. Inducing changes in the electronic transparency of this molecule is discussed in Sec. III, and then applied in Sec. IV to a dimer of benzene molecules and a C_{60} molecule. Details of the molecular level shifts involved are provided. The transistor effect is presented in Sec. V, again using a single C_{60} molecule in compression. New opportunities and future directions for further development are stated in the conclusion.

II. TUNNEL TRANSPORT IN A MOLECULE

A molecule positioned between the source and the drain as in Fig. 1 is certainly better than vacuum for closing an electrical circuit. This was clearly demonstrated experimentally by comparing the current intensity (measured using a standard amperemeter) between a vacuum tunnel junction and the same junction ''short circuited'' by a molecule.[9] Even saturated molecules such as alkane chains are several orders of magnitude better than vacuum for a given interelectrode separation.[10]

The tunnel process through a molecule arises from the electronic interactions between the molecule, the source, and the drain electrodes in what is a strongly coupled system. The net consequence of those interactions is an extension of the metal electronic wave functions outside the metal along the molecule compared to their rapid falloff in vacuum. This extension has recently been measured by scanning an STM tip along the molecular axis of a designer molecular wire connected on one side to a step edge.[11]

In a molecule, the opening of alternate tunnel channels results from the overlap of the metal wave functions spreading through the molecule. Both drain and source contribute to the extension of the metallic wave functions. Their significance can be appreciated from the resultant broadening of the molecular levels involved.[12] This is much larger than in their free state[13] (gas phase). It is measured by the exponential decrease of the current intensity along the length of the molecular wire when connected to only one electrode.[11] In this case, an exponential dependence $I_d = I_0 \exp(-2\gamma x)$ prevails, where the inverse decay length γ is related to ϕ through the relation $\phi = 4\gamma^2$, with ϕ in eV and γ in $Å^{-1}$. This yields a molecular ϕ consistently lower than that for the equivalent vacuum gap.[11]

Under resonance conditions with predefined molecular levels, the overlap of the tails of the metal wave function and the molecule results in further delocalization. This occurs at certain energies. The resulting process, however, is rather unstable owing to the low density of levels in a molecule compared to a solid-state sample (even a mesoscopic one). In contrast, within the HOMO-LUMO energy gap χ, many tunnel channels can effectively contribute to the formation of a drain-to-source tunnel path via the molecule. These channels arise not only from the HOMO and LUMO levels but also from other molecular levels the widths of which are significantly enlarged such that they span the HOMO-LUMO gap.[12] The superposition of these new tunnel channels may not always result in a constructive phenomenon. Differences in symmetry between the molecular orbitals involved can also result in a destructive interference, itself an interesting physical phenomenon usable in nanoelectronics. The efficiency of tunnel-channel superposition can be evaluated in a similar manner as ballistic channels in mesoscopic physics[14] by the transparency $T(E)$ of the tunnel path. This is a normalized average of all the transmission coefficients of the metallic electron Bloch waves scattered by the drain-molecule-source double junction.[12] A resulting $T(E)$ spec-

trum is calculated by constructing a scattering matrix[12] and estimated experimentally by measuring the macroscopic resistance of the drain-molecule-source double junction using the Büttiker-Landauer formula.[15] In this scheme, $T(E)$ depends on the energy of the incident electron and on the source-drain voltage V_{ds} across the molecule.

At $V_{ds}=0$, the molecular levels are normally occupied up to the HOMO closest to the Fermi level E_F of the nanocontact. The density of states between this level and E_F is nonzero owing to a broadening of the molecular level width. For the molecules considered here, a significant electron density is available at E_F in the molecule for transporting tunneling electrons.[13] This supplementary electron density is facilitated by the spreading of the metallic electron wave functions through the molecule itself. Importantly, at small HOMO (or LUMO) separations from E_F, holes (electrons) can be thermally activated onto a corresponding molecular level. Supported only by discrete levels, this thermal current is extremely sensitive to voltage fluctuations, molecular conformations, and adsorption configurations. For nanoelectronically dense fabrication, these usually represent undesired effects. However, in the molecular devices discussed here, they can readily be suppressed by engineering a sufficiently large HOMO-LUMO gap with respect to kT to circumvent such electron-phonon coupling.

The drain-current intensity I_d depends on the molecular length, chemical composition, and—very crucially—on the conformation (shape) of the molecule that forms the active ''molecular'' channel between source and drain. In the energetic window $eV_{ds} \ll \chi$, the $I_d(V_{ds})$ characteristics of such junctions are theoretically predicted and experimentally verified to be linear because the energy of the tunneling electron is within the HOMO and LUMO resonances. This is a molecular equivalent to the ''Simmons'' condition for metal-vacuum-metal tunnel junctions.[16] It is required for establishing tunneling transport through ''molecular'' channels.[17] Here the electrons are transferred one at a time. The transit time through such a molecular channel is shorter than the time $t=e/I_d$ between two electrons delivered by the source-to-junction channel.[18] This transport mechanism will remain elastic as long as the transit time remains shorter than the characteristic intramolecular relaxation time. Inelastic channels develop only when the molecule is sufficiently long for the transit time to approach the relaxation time. This basic limit can be understood in terms of the transit (tunneling) time through a molecular channel, which is proportional to $\exp(+2\gamma L)$, where L is the length of the channel.[19] An optimum choice of the molecular length therefore permits the elastic tunneling transport regime to be the dominant conduction mechanism.

Basic design rules to establish the tunnel path through a molecule can be developed by modeling the molecule as two principal molecular levels involved in the tunneling process: Its HOMO and LUMO levels are then allowed to interact with two one-dimensional (1D) electrodes representing source and drain nanocontacts. For example, if the HOMO is symmetrically and the LUMO antisymmetrically coupled to the electrodes, each level opens a tunnel channel (Fig. 2). Their superposition in the HOMO-LUMO energy range will be constructive due to the symmetry chosen in this case. This situation features the tunnel-path formation in a real

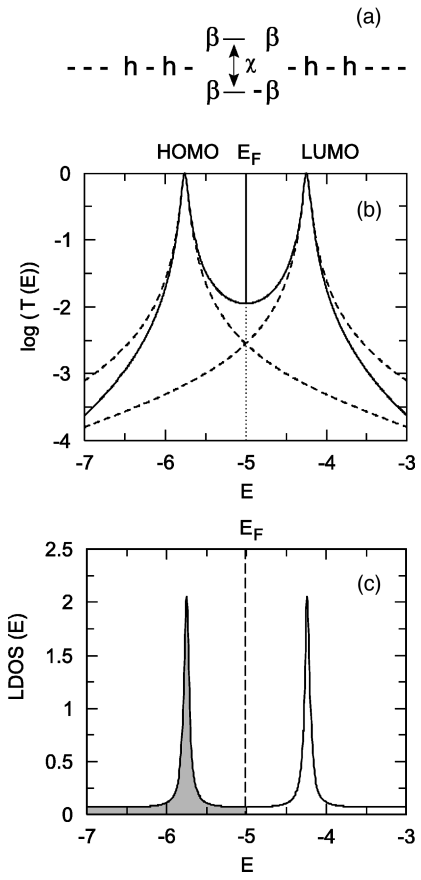

FIG. 2. Variation of the transparency $T(E)$ and the local density of states LDOS(E) as a function of the incident energy of the electrons scattered elastically by a two-level system with a separation of $\chi=1.5$ eV. Here the contact Fermi level is at $E_F=5$ eV, and the electronic coupling between the two-level system and the 1D electrodes is $\beta=0.2$ eV, with a resonance integral $h=2$ eV along the chain representing the 1D electrodes. (a) Tight-binding presentation of the calculated system. (b) $T(E)$ spectrum. The Lorentzian dashed lines are from the same spectrum, but with only the HOMO or the LUMO level activated. (c) LDOS(E) spectrum with the occupied states indicated.

molecule.[12] The transparency $T(E)$ and the change in local density of states LDOS(E) introduced by the two channels are presented in Fig. 2 and calculated using a standard tight-binding representation.[20] In a first step, the spatial propagator 2×2 matrix along this 1D chain was calculated. In a second step, the 2×2 scattering matrix was obtained. $T(E)$ is the modulus of the first element of this matrix and LDOS the derivative of its argument.[20]

The values used for the ''electrode-molecule'' electronic coupling β and for χ in Fig. 2 are characteristic of a low HOMO-LUMO gap conjugated molecular wire. At E_F, the transparency of the tunnel path resulting from the constructive superposition of the HOMO and LUMO tunnel channels is approximately 10^{-2}, which leads to a resistance of 1 MΩ. This is a typical value for a short, conjugated molecule ($L \approx 1$ nm) with a decay length γ^{-1} not yet stabilized and representative of an optimally chemisorbed molecular contact on source and drain.

Here the LDOS indicates a moderate enlargement of the HOMO and LUMO level width towards E_F. The $I_d(V_{ds})$

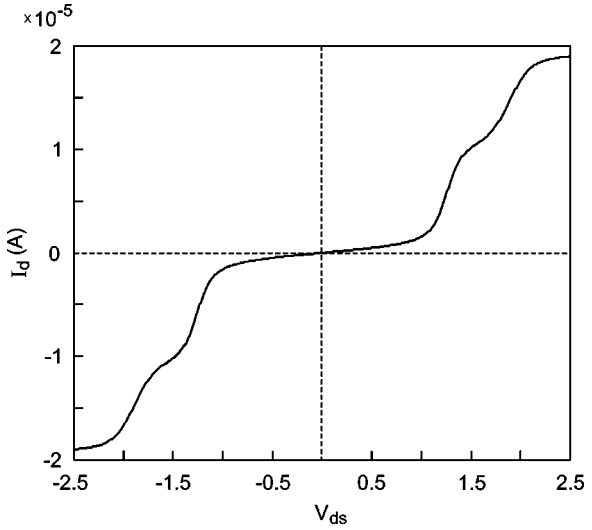

FIG. 3. The calculated $I_d(V_{ds})$ characteristic of the two-level system in Fig. 2(a), revealing the linear-law voltage part for $V_{ds} < \chi$ and a stepped structure when the bias voltage $V_{ds} > \chi$. $I_d(V_{ds})$ was calculated taking an effective electric-field level shift of 0.4 V_{ds} into account (Ref. 21) to show the multiple steps that appear even if there is no Coulomb blockade and only two levels in the system.

characteristic presented in Fig. 3 is linear for $|V_{ds}| < 0.5$ V. For large values of V_{ds}, I_d was calculated by integrating $T(E)$ over the difference of the Fermi distributions of source and drain electrodes, shifted by eV_{ds} relative to each other, at $T = 300$ K, and assuming a 1D density of states in those electrodes. For low values of V_{ds}, this leads to the standard linear approximation $I_d = (e^2/\pi\hbar)T(E_F)V_{ds}$ used in the following even for a multichannel calculation of $T(E)$. The stepped structure is the signature of eV_{ds} as it reaches the HOMO (or LUMO) level. With increasing energy, the appearance of a 1-eV gap around $V_{ds} = 0$ is actually the result of an enlargement of the molecular levels introduced by β because $\chi = 1.5$ eV in the calculation.

The transit time through this simple but illustrative molecular structure can now be estimated by calculating the electron transfer rate of a four-level system comprising an input and an output state with two intermediate HOMO and LUMO levels. This transfer rate can be expressed as $\nu = \chi h^{-1}\sqrt{1+4\beta^2\chi^{-2}}$, which yields a transit time of 10^{-16} s.[22] To put this value into perspective, the average time interval between two electrons delivered by the source to this four-level system can be estimated from the Landauer formula, $I_d = (e^2/\pi\hbar)T(E_F)V_{ds}$, to yield a duration of $e/I_d \approx 10^{-12}$ s.

The clear implication for a short molecular channel with a 1.5-eV HOMO-LUMO gap, characterized by a reasonable 10^{-2} transparency, is that the transport regime in the channel occurs by tunneling with an average of one electron transiting the tunnel path per unit of time. With respect to Coulomb blockade effects, our calculations show that, in this transport regime, the electrons do not charge the molecule. In the linear ''molecular-Simmons'' I-V regime of a double junction, the molecule is, in principle, only virtually occupied by the transiting electrons. This is a general consequence of virtual resonance tunneling (VRT) where the transit time is very short. The Coulomb blockade effect is thereby avoided and a linear $I_d(V_d)$ characteristic is maintained by operating in a pure quantum regime.

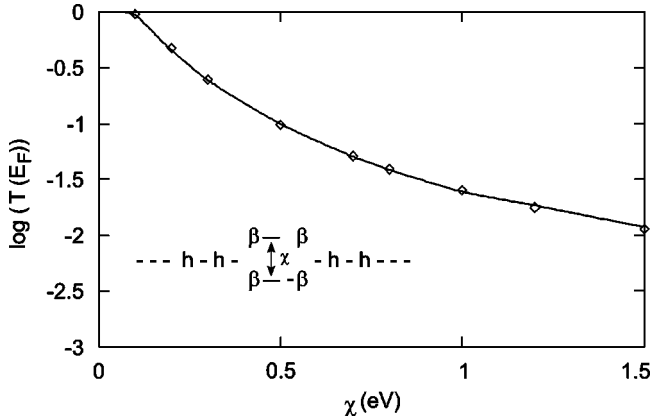

FIG. 4. Variation of the transparency of the two-level system in Fig. 2(a) as a function of its HOMO-LUMO gap χ for a fixed value of $\beta = 0.2$ eV. This transparency is calculated from the low-voltage Landauer formula giving the conductance I_d/V_{ds} of the junction as a function of χ.

III. ACTING ON THE MOLECULAR CHANNEL TRANSPARENCY

The transparency of a molecular channel depends on the spreading of the metal wave function over the molecule embedded in the source-molecule-drain junction. Retraction or extension of the metallic wave function from the molecule at both sides (source and drain) will reduce or increase the tunneling-current intensity, respectively. We foresee that these effects can be utilized to create an intramolecular valve action. Conceptionally, this may also exist between subcomponents of a single molecule, independent of the metallic electrodes, but this is more challenging to put into operation at present.

The change in the spreading of a wave function along a molecule's length has been the subject of much research. Intramolecular through-bond electron transfer experiments[23] have provided insight into how intramolecular conformation changes[24] or chemical modifications[25] can practically preclude electronic communication from one end of a molecule to the other. For instance, the HOMO (or LUMO) molecular levels are shifted by such intramolecular transformations.[26] The resulting changes in the rate of intramolecular electron transfer are direct proof that sufficient degrees of freedom are available in a molecule for the coherent control of the electron-transfer process. Sequential electron transfer through a molecule under the VRT transport regime implies that intramolecular modifications determine the transparency of the intramolecular channels.

In our fundamental model (Fig. 2) of a molecular channel, any reduction of χ increases the transparency of the channel as it increases the through-bond electron-transfer rate.[26] The $I_d(V_{ds})$ characteristics of such channels remain linear for $V_{ds} \ll \chi$. Their slope follows variations in χ. However, the conversion between χ and transparency amounts to only one order of magnitude per 1 eV reduction of χ (see Fig. 4). Here we note that reducing χ does not change the width of the level supporting the tunneling current but only its relative

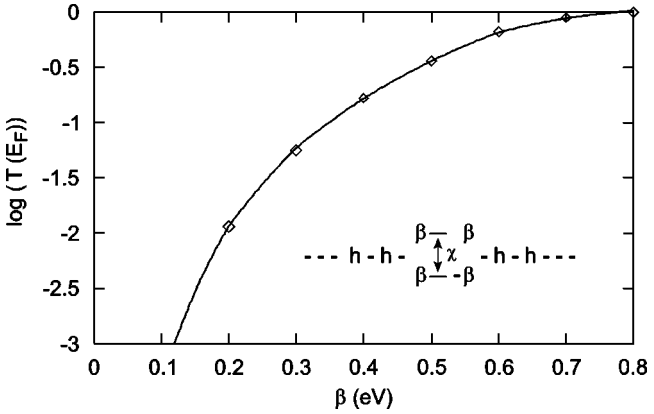

FIG. 5. Variation of the transparency of the two-level system in Fig. 2 as a function of its electronic coupling to the 1D electrodes for a fixed $\chi = 1.5$-eV HOMO-LUMO gap. The transparency has been calculated in the same way as in Fig. 4.

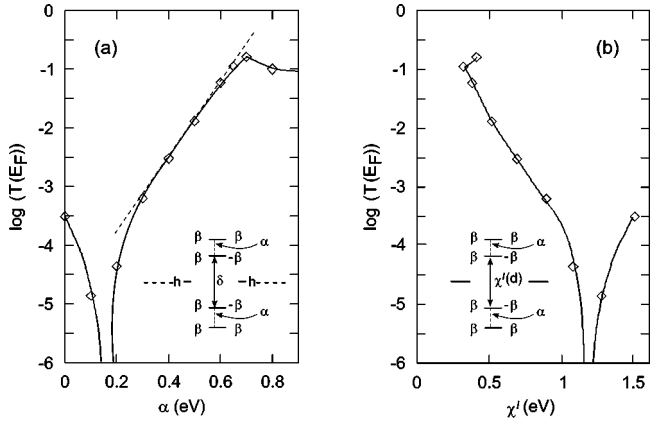

FIG. 6. (a) Variation of the transparency of the four-level system shown in the inset as a function of the intramanifold electronic coupling α for $\beta = 0.2$ eV and $\delta = 0.3$ eV. For $0.3 < \alpha < 0.7$ eV, this transparency is almost exponential in α, as indicated by the dashed line. This is a particular property of the effective electronic coupling through this four-level system. (b) Same variation as in (a) but as a function of the HOMO-LUMO gap χ' controlled by α with $\chi' < \chi$ for $\alpha \neq 0$.

position. Furthermore, a reversible change of the HOMO-LUMO separation by 1 eV is difficult to achieve without actually modifying the chemical structure of the channel. Such a change appears unrealistic for the grid of a single molecular transistor. A far better conversion is obtained by considering the β term instead of the χ term in Fig. 4, as presented in Fig. 5. Unfortunately, this is not an intrachannel effect, as is the χ effect, but rather depends on the manner in which the molecule is chemically docked to the source and the drain.

The key point of the amplifier and transistor device discussed here, namely, level-repulsion phenomena, can now be introduced. The closure of the HOMO-LUMO gap is achieved indirectly. By changing the electronic coupling inside the HOMO and the LUMO manifolds themselves, key features of a single molecular amplifier can be obtained. This requires the channel to have a more complex intramolecular structure than a two-level system because the dimension of the manifolds must be greater than unity for a repulsion to occur.

Consider a molecular tunnel path having four levels: two degenerated HOMO's and two degenerated LUMO's. In each manifold, molecular levels are symmetrically and antisymmetrically coupled to the nanocontacts as represented in Fig. 6. In the absence of additional coupling, it can be shown that the transparency of this four-level system is uniformly zero over the entire energy range. This results from the reciprocal annulation of the effective coupling between the various tunnel channels opened by those four levels. The introduction of a small HOMO-LUMO intermanifold electronic coupling δ restores the nonzero transparency of the tunnel path. More importantly, for $\delta \neq 0$ the introduction of even a minute intramanifold electronic coupling, α, results in a very large transparency change. Figure 6 demonstrates, for instance, a change of more than two orders of magnitude for an input variation of less than 0.3 eV in α. The explanation of the high sensitivity presented by the transparency is that α introduces a strong intramanifold level repulsion resulting from the initial degeneracy of the levels in each manifold. It is amplified by a zero of transparency for $\alpha = \delta/2$. Such a repulsive effect constitutes the physical background for operation of the C_{60} amplifier.

Tunneling through a four-level system with $\delta \neq 0$ and $\alpha \neq 0$ is equivalent to tunneling through a nondegenerate, uncoupled four-level system obtained by diagonalizing the former. The equivalent system has a HOMO-LUMO separation χ', which is a function of α and δ. The effective electronic coupling between this four-level system and the nanocontacts is also a function of α and δ. With the channel structure, Fig. 6, we have consolidated both the χ variation presented in Fig. 4 with the β variation presented in Fig. 5. Overall the modeling indicates that optimum operation requires predefined intramolecular electronic structures for the respective channels. These are quite distinct from those proposed for molecular wires[12] and differ from simple combinations of molecular nodes usually proposed in the literature for obtaining a transistor effect in a molecular circuit.

The simple tight-binding model used here demonstrates that a large transparency variation of a molecular tunnel path can be obtained with a small perturbation of its intramolecular electronic structure. Four channels appear to represent the minimum number of levels required in the path to attain such a sensitivity.

In the schematic in Fig. 1, the molecule is gated by a third electrode, independent of the source-drain distance L. According to the results presented in Fig. 6(a), there is a range of α in which I_d grows exponentially upon a linear variation in α with β kept constant, i.e., with fixed L. In this range, the current can be written in a first approximation from its transparency [see Fig. 6(a)] as

$$I_d = i_0(V_b) e^{k\alpha(V_g)}, \tag{3}$$

where i_0 is a prefactor depending on L, γ_0, and on the way the molecule is chemically bound to the electrodes. The active part of the channel is no longer controlled by γ_0 because L is constant. There is still an exponential term $e^{-2\gamma_0 L}$ in $i_0(V_b)$ because if L is changed, I_d must change too. But this is an interface factor indicating how the metal wave functions match those of the molecule. Using Eq. (2), we find

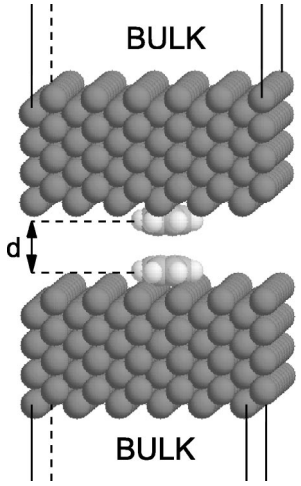

FIG. 7. Schematic of the tunnel-junction configuration having two face-to-face benzene molecules to reproduce a simple level-repulsion effect. The tunnel-current intensity through this junction was calculated using the STM-ESQC technique (Ref. 27).

that the gain of such a device relies on the slope $kd\alpha(V_g)/dV_g$, where k is characteristic of the molecule used. As will be demonstrated below, the real difficulty we solved was to find a way with $\alpha=\alpha(L)$ and $L=L(V_g)$ to act on the intramanifold-repulsion parameter α using a third electrode.[1,9]

IV. LEVEL REPULSION DURING C_{60} COMPRESSION

The proposed four-level repulsion effect exists even within simple molecules. Let us first consider two benzene molecules, each adsorbed on a flat surface as presented in Fig. 7. As a working example, it provides a useful system to use efficiently our elastic scattering quantum chemistry (ESQC) technique[27] to calculate the conductance of a metal-benzene benzene-metal double tunnel junction. The HOMO and LUMO manifolds of two face-to-face noninteracting benzenes are each of dimension 4. Two π symmetrical and two π antisymmetrical orbitals per manifold are coupled to the electrode electronic levels. This represents twice the channels necessary to achieve an intramolecular level-repulsion effect. Through-space δ and α electronic couplings are very small at large distances such that the junction transparency with the dimer is zero when the HOMO-LUMO gap becomes constant.

The benzene-electrode coupling is defined by a benzene-to-surface distance of 2.3 Å. Although this is large compared to standard chemisorption distances, the repulsion effect will soon become apparent in a $T(E)$ spectrum. The mechanical compression effect is modeled by progressively reducing the interbenzene distance z in the dimer, maintaining each benzene-to-surface distance constant. As the distance decreases, the intermanifolds and intramanifold's electronic coupling increase. Below $z=3.4$ Å, the energy of the dimer is observed to increase considerably, illustrating that an external force must be applied to the electrodes to maintain the dimer at the set distance. Contrary to the tight-binding system in Fig. 6 where δ and α can be chosen independently, on a real molecule the two interactions are intimately associated, where δ and α change in conjunction.

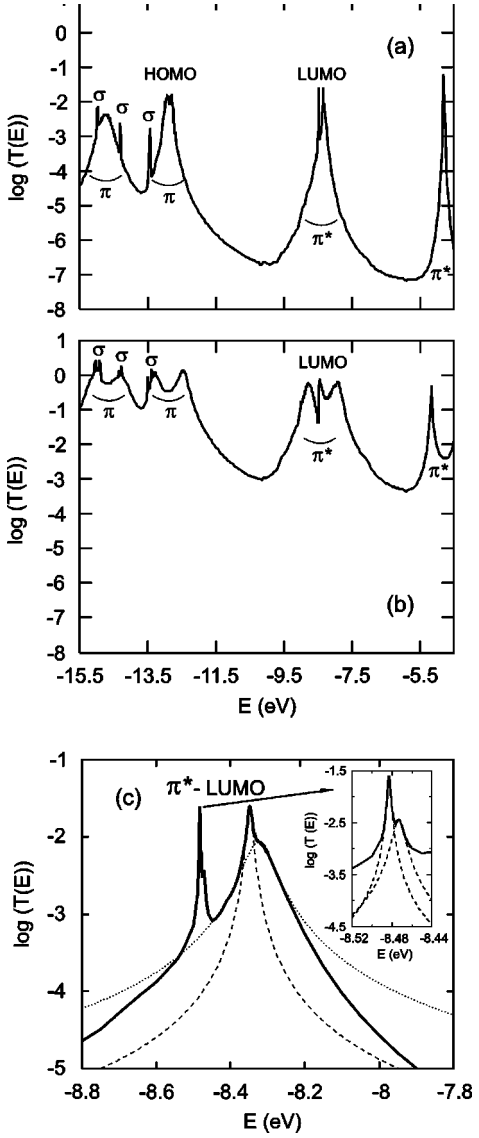

FIG. 8. The $T(E)$ spectrum for the tunnel junction presented in Fig. 7 having two benzene-molecules for a benzene-benzene distance of (a) 5 and (b) 3 Å. (c) Closeup of the spectrum in (a) around the LUMO manifold where the four π^*-level resonances are clearly visible. Each level defines a tunnel channel with its own resonance width depending on the corresponding molecular orbital electronic coupling with the metal surface. Each Lorentzian π^* resonance is indicated by a dashed line.

The $T(E)$ spectra for $z=5$ and 3 Å are presented in Fig. 8. For example, at $z=5$ Å, the LUMO manifold as shown in Fig. 8(c) displays four structures, corresponding to the four π LUMO levels. At $z=5$ Å, each benzene is a short (2.3 Å) distance from its own surface. However, they are both 7.3 Å apart, hence they are not in resonance. The tunnel barriers exhibit asymmetry, which constrains the maximum of the transparency to remain below unity. The remaining features are readily identified as deeper occupied and higher unoccupied σ and π molecular orbitals of the benzene dimer. At $z=3$ Å, level repulsion occurs: two levels move up and two levels move down in each manifold, as we intuitively expected. In this case, the HOMO-LUMO separation is reduced by 0.6 eV. The consequence of this mechanoelectronic effect is an increase of electronic transparency of almost four or-

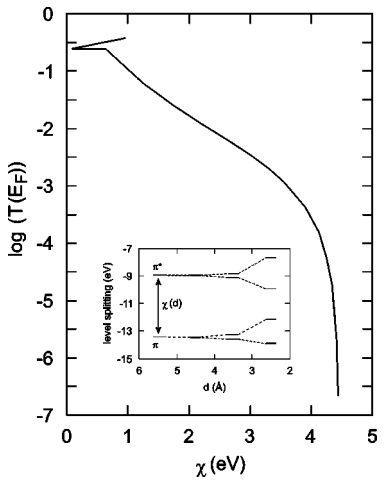

FIG. 9. Variation of the transparency of the dimer benzene junction shown in Fig. 7 as a function of its HOMO-LUMO gap. This curve compares well with that in Fig. 6(b) in the $\chi<1.1$ eV range, before the zero in transparency. Inset: schematic of the level-repulsion effect. Only the HOMO and LUMO manifolds are represented.

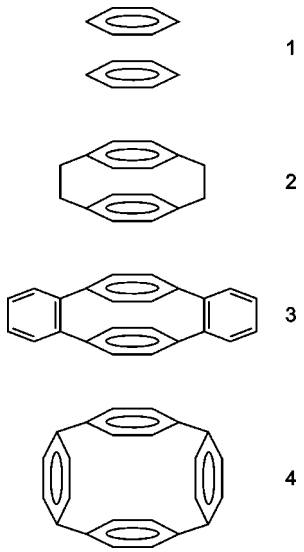

FIG. 10. Examples of (1) a benzene dimer in a parallel configuration calculated from the junction in Fig. 7, (2) a cyclophane molecule (Ref. 28), (3) with the phenyls maintained face-to-face by the other two lateral ones (Ref. 28), and (4) an element of a picotube (Ref. 29).

ders of magnitude. This provides a very satisfactory performance of two orders of magnitude change in current per angstrom of compression. To confirm the level-repulsion effect, we have plotted in Fig. 9 the transparency of the dimer as a function of the HOMO-LUMO separation estimated from the calculated $T(E)$ spectrum. This curve is almost identical to the one presented in Fig. 6, except that the zero of transparency is pushed towards the natural HOMO-LUMO gap of the molecule. As previously stated, this lends support to our argument that, in a real molecule, δ and α are inseparably linked.

In an STM junction, it has not been demonstrated that two benzene molecules in parallel orientation—one on the tip and one on the surface—can yet be realized. Theoretically we have chosen to explore the repulsion effect and its sensitivity, where the two partners of the interaction are chemically fixed. Starting from this benzene dimer, there are many further molecules or architectures available that respect similar constraints. As shown in Fig. 10, a cyclophane molecule (2) maintains two benzene rings at a distance of 3.4 Å using saturated ''connectors.'' Conjugated arms such as phenyl components (3) or even a unit of the recently proposed picotube molecule (4) also maintain two face-to-face benzenes, despite some distortion. To achieve a high degree of transparency through these dimers, conjugated connectors appear to be electronically preferable to saturated connectors. Furthermore, the adsorption conformation of the molecule on the substrate should ideally favor a planar-to-surface benzene conformation. Our choice of C_{60} having many face-to-face phenyl groups, for which the intervening chemical structure is clearly not saturated, appears well suited in light of the preceding model system. Moreover, its HOMO manifold has a dimension of 5 and its LUMO a dimension of 3, an ideal condition for molecular level repulsion.

The variations of the C_{60} transparency under compression are calculated more realistically than with the benzene dimer. One electrode was equipped with a tip apex and the entire geometry of the cage was optimized for each tip apex-to-surface distance z. The conductance of the ''metal electrode-tip apex-C_{60}-metal surface-metal electrode'' tunnel junction was then calculated using the ESQC technique for each conformation, the entire valence structure of the C_{60} molecule being taken into account.[9] Details of the transparency spectrum are given in Fig. 11 from $z=13.85$ to 11.35 Å. A level-repulsion effect clearly occurs when the C_{60} cage is compressed by the tip apex as shown in Fig. 12 by plotting the C_{60} transparency as a function of the HOMO-LUMO separation. This is confirmed experimentally as the C_{60} intramolecular mechanics and electronic reorganization due to compression have been obtained by plotting the $I_d(z)$ characteristics.[9] This experimental result is well reproduced by the same calculation scheme that we used to calculate the $T(E)$ spectrum (Fig. 11) and the dependence of $T(E_F)$ on the C_{60} HOMO-LUMO gap (Fig. 12).[9] The sensitivity of the level-repulsion effect to compression compares well with that of the benzene dimer (Fig. 9) and with our simple tight-binding model (Fig. 6).

For $z>14$ Å, there is no compression of the C_{60} cage and again $I_d(z)=I_{C_{60}}\exp-(\sqrt{\phi}z)$ with $\phi=4\gamma_0^2=5$ eV as found experimentally.[30] The $I_{C_{60}}$ factor is different from the prefactor in Eq. (1) because a C_{60} molecule in the tunnel junction brings several orders of current intensity more than the vacuum.[9]

In the compression range, 10.7 Å$<z<$12 Å, the tunnel-current intensity at the center of the HOMO-LUMO gap can be fitted by the expression

$$I_d(z)=I_{C_{60}}e^{-(\sqrt{\phi}+K_{C_{60}})z}, \tag{4}$$

which can be obtained from the experimental $I_d(z)$ results or by using the calculated ESQC data.[9] The role of $\sqrt{\phi}$ in Eq. (4) is standard, and has already been discussed in the introduction. The $K_{C_{60}}$ term is new. It results from the level-repulsion effect. Compressing the C_{60} cage introduces an in-

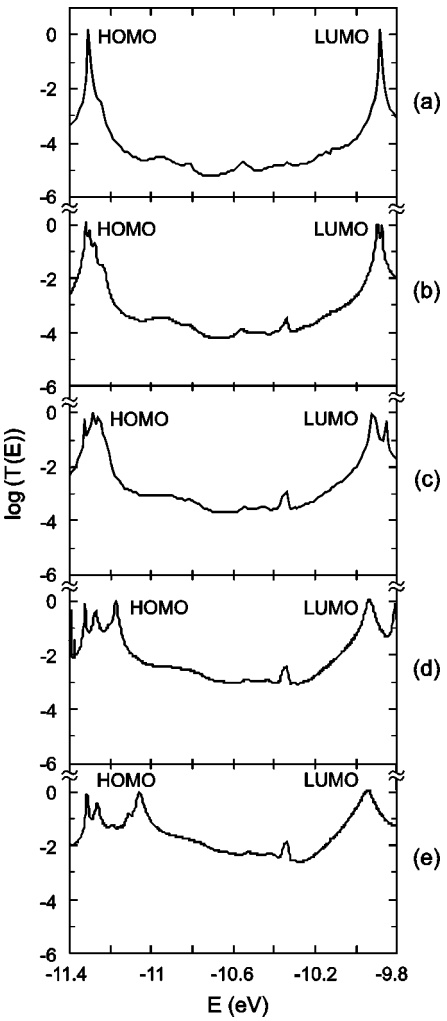

FIG. 11. $T(E)$ spectra for a single C_{60} molecule compressed by the STM tip apex. The tip apex-surface distance is (a) 13.85, (b) 13.35, (c) 12.85, (d) 11.85, and (e) 11.35 Å. Only the HOMO-LUMO gap region is represented.

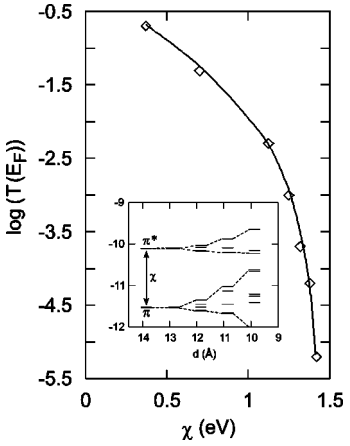

FIG. 12. Variation of the transparency of the C_{60} molecule compressed by the STM tip as a function of its HOMO-LUMO gap. The latter is calculated as shown in the inset, i.e., by recalculating the C_{60} compressed electronic structure as a function of the tip apex-surface distance. This curve compares well with the one in Fig. 6(b) for $\chi<1.1$ eV and with the benzene-dimer curve in Fig. 9.

tramixing of the levels in the HOMO and LUMO manifold (see Fig. 12). Then, their intramanifold degeneracy lifts, followed by the C_{60} HOMO-LUMO gap closure, as shown in the inset of Fig. 12. This gap change quantitatively controls the overlap on C_{60} of the evanescent metallic waves emanating from both the tip apex and the surface electrode. This is not taken into account by the $\sqrt{\phi}$ exponential term in Eq. (4), which characterizes only the through-space penetration depth of this evanescent regime.

The formal $\alpha(V_g)$ function introduced in Eq. (3) is here a linear $K_{C_{60}}z$ function of z, with $z=z(V_g)$. For the range $10.7<z<12$ Å, comparison with experiment[9] (and with calculations) yields $\sqrt{\phi}+K_{C_{60}}=5.31$ Å^{-1}, i.e., $K_{C_{60}}=3.07$ Å^{-1}. This triggered the search for a molecule with a better manifold intramixing for a moderate compression of the molecule.

We have experimented with the transductance of the amplifier by directly applying V_g on the z-piezo-tube of an STM tip.[1] This indirect gate on the piezotube was the only means at hand to gate the C_{60} channels,[9] and to prove that a gain can be obtained with a single molecule using its intrinsic electronic structure. Using a piezo with a conversion factor of 1 Å/10 mV, the extracted value of $\sqrt{\phi}+K_{C_{60}}$, and a set distance of 11.7 Å,[9] the normalized transconductance of our amplifier is given by Eq. (2) by $g/I_d=531$ V^{-1}. This value is more than twice that of a vacuum tunnel junction. For $V_b=0.2$ V, $I_{C_{60}}$ in Eq. (4) is found to be 7.48 nA in the experimental $I_d(z)$ characteristics,[9] confirming the low working current of a nonresonant tunneling device as discussed in the Introduction. For a load of 10^6 Ω, the gain of this amplifier with a piezotube gate is $g\times10^6\approx4$.[1]

V. ELECTROMECHANICAL SINGLE-MOLECULE TRANSISTOR

Fabricating the source and drain electrodes on the same surface of a semiconductor material as the transistor channel was the key to advance from the first point-contact transistor to a state-of-the-art integrated circuit.[31] The same planarization step for the C_{60} amplifier allows the separation of the grid[2] as proposed in the schematic in Fig. 1. Furthermore, the amplification arises here from the level-repulsion effect. This effect is not solely restricted to C_{60} molecules as shown in the preceding section. It requires molecules with degenerated HOMO and LUMO manifolds. Therefore, a planar version of the C_{60} amplifier will also open the number of molecular systems to those not accessible to compression under an STM tip apex.

The planar setup of the C_{60} amplifier is straightforward to design.[2] The ''tip-apex-C_{60}-molecule-surface'' junction is planarized in a ''metal-C_{60}-metal'' nanojunction fabricated on top of an insulating material. The grid can be mechanical but also electrical. An electric field applied transversally to this planar junction will mix the ground and excited molecular levels of C_{60} (an equivalent of the δ electronic-coupling term introduced in Sec. III). With an appropriate orientation of the field with respect to the molecular axis, the manifold degeneracy can be lifted (the α effect). However, the effect of an electric field at present appears to be generally minor at the molecular level compared to a local microscopic field. As

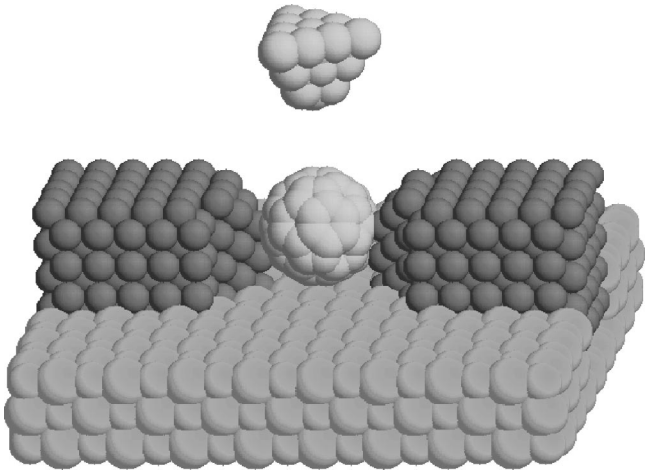

FIG. 13. Schematic of the planar version of the C_{60} amplifier. The electromechanical grid is separated from source and drain. The tip apex consists of insulating material and is supposed to be supported at the end of a cantilever (Refs. 2 and 33) (not shown here) that is equipped with a piezolayer to control its deflection. The separation between the two metallic pads must be less than 1.5 nm to allow operation in the nanoampere range.

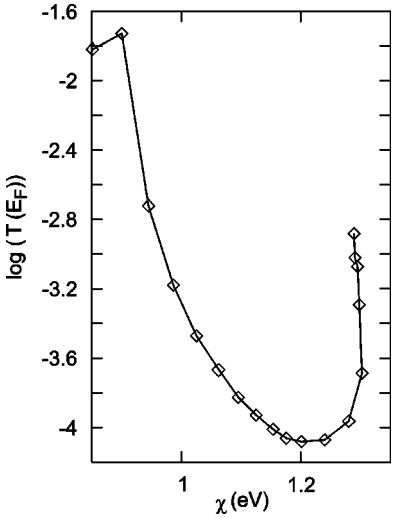

FIG. 14. Variation of the transparency of the C_{60} molecule in the junction configuration presented in Fig. 13 as a function of the effective C_{60} HOMO-LUMO gap. This gap changes as a function of the altitude of the grid tip apex. It was calculated after a full optimization of the atomic configuration of the junction in Fig. 13. Note the $T(E_F)$ minimum due to the zero of the transmission effect presented in Fig. 6(b).

such, it obliges one to work with high-field strengths, which are generally incompatible with the stability of nanocontacts.

Mechanical effects are more amenable to nanoscale experiments because the local forces applied by a tip apex on a single adsorbate compete well with the strength of intramolecular bonds.[32] Therefore, we have chosen a microcantilever positioned on the nanojunction for the grid to compress gently the C_{60} cage from the top[2] (Fig. 13). This cantilever is deflected by a piezolayer deposited on its top face. The technology to realize such a design has been discussed recently together with the competition between the piezolever sensitivity and its resonance frequency when the cantilever dimensions are reduced to 0.1 μm.[33] Here we focus only on the electronic characteristics of the planar device shown in Fig. 13.

The ESQC technique was used to calculate its source-drain tunneling-current intensity as a function of the cantilever apex to surface distance z when the cantilever end is positioned vertically above the C_{60} molecule. As done previously, the mechanics of the junction was optimized using the MM2 routine. The source and drain are two gold electrodes of 25 atoms each in section, and semi-infinite in one direction. At the junction, each end of the electrode is not flat but rather terminated by an apex to optimize the electronic coupling between these electrodes and the C_{60} HOMO and LUMO manifolds. The two electrodes and the C_{60} molecule are deposited on a rigid NaCl surface. The interelectrode distance L is 1.24 nm. This is the optimum distance to obtain a good electronic contact between the electrodes and the C_{60} molecule, as determined experimentally and by calculations.[9,17] For $V_{ds}=0.2$ V and $V_g=0$ ($z>14$ Å), the calculation yields $I_d=15$ nA for the device shown in Fig. 13. The lever end consists of a diamond tip with (111) facets, previously used for the calculation of atomic-force microscopy images.[34]

As described in Sec. IV, a compression of the C_{60} cage results in a strong intra-HOMO and LUMO manifold-repulsion effect. But this effect depends on the horizontal (Fig. 13) and vertical way the current is measured. For vertical access,[9] the junction transparency is zero when the tip is far away from the molecule. For a horizontal configuration (Fig. 13), there is a net residual current in the absence of compression because the interelectrode distance is fixed. Therefore the inter-HOMO-LUMO δ-like interaction via the surface of the electrodes is much larger than in the vertical case. Hence, and according to Fig. 6(b), there must be a zero of transmission for a given value of χ. The $T(E_F)$ variations as a function of the C_{60} HOMO-LUMO gap under compression is presented in Fig. 14 for the arrangement shown in Fig. 13. There is a small (0.1 Å) increase in the diameter of the C_{60} cage when the grid apex approaches C_{60} in a weak attractive van der Waals regime. This explains the small gap increase around $\chi=1.3$ eV. When compression sets in, χ and $T(E_F)$ decrease, as expected for $\delta\neq 0$ [see Fig. 6(b)]. But $T(E_F)$ does not attain zero because in the C_{60} molecule more tunnel channels than the HOMO and LUMO ones are active. Some of the other channels are spectrally rigid and maintain their contribution to the tunnel path. At larger compression, the gap continues to decrease and $T(E_F)$ starts to increase.

The $I_d=f(z)$ characteristic is presented in Fig. 15. For $z>12.5$ Å, the residual set current is 7 nA for $V_b=0.1$ V. For $10.5<z<12.5$ Å, the current intensity decreases owing to the zero of the transmission effect. For $10<z<10.5$ Å, there is a large increase in I_d for a minute reduction of z. This is the signature of a strong level-repulsion effect with a change of the C_{60} HOMO-LUMO gap. In this planar configuration, this effect mainly stems from the HOMO manifold split by the compression of the cage. For $z<9$ Å, C_{60} is so strongly compressed that it escapes from the junction.

In the range $10.0<z<10.5$ Å, I_d increases exponentially for a small z variation. An amplification results as in the vertical STM configuration. In this range, the mechanical

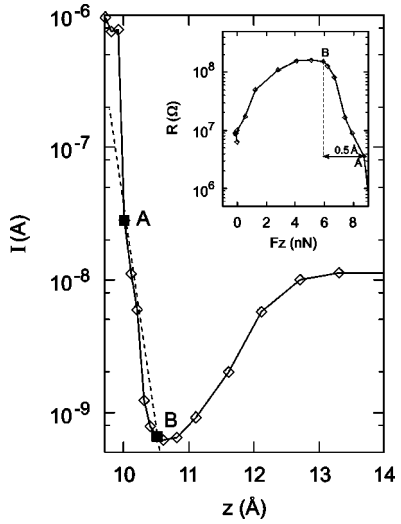

FIG. 15. Variation of the drain current I_d in the source-C_{60}-drain junction presented in Fig. 13 as a function of the distance between the diamond tip apex and the NaCl surface z with $V_b = 0.1$ V. The mechanical contact between tip apex and C_{60} surface occurs at $z_0 = 12$ Å. For $10 < z < 10.5$ Å, the current can approximately be fitted by the dashed line giving the exponential law in Eq. (5). On this line, *A* and *B* are the optimal working points of the device, with *A* its low- and *B* its high-impedance state. The inset shows the source-drain Ohmic resistance as a function of the force applied to the C_{60} cage by the tip grid. From this curve, an ''on (A)–off (B)'' minimum switching energy of 1.25×10^{-19} J is deduced.

potential energy of the junction increases by 50 kcal/mol. As shown in Fig. 15, the $I_d(z)$ characteristics can almost be fitted by the exponential

$$I_d(z) = I_{d_0}(V_b) e^{-k_{C_{60}} z}, \tag{5}$$

where $k_{C_{60}} = 7.505$ Å^{-1} is the level-repulsion sensitivity of the device.

Contrary to Eqs. (1) and (4), the exponential variation in Eq. (5) is due solely to the intramolecular effect. This is a clear exploitation of the intrinsic property of a molecule to obtain a gain on the nanoscale. By building an effective squared tunnel barrier to model this molecular device, we can control the barrier height by a third electrode, but in a linear $I_d(V_b)$ regime. This clearly constitutes a transistor effect because the transfer resistance through the effective barrier between the source and drain electrodes is controlled by the intrinsic property of molecular channels, themselves modulable by a third independent mechanical electrode. With a 1 Å/10-mV piezoconversion factor, the normalized transconductance of this transistor is $g = 750$ V^{-1} with a small ($I_{d_0} = 0.66$ nA) prefactor compared to Eq. (4) but at $V_{ds} = 0.1$ V.

VI. CONCLUSION

The principle of our C_{60} electromechanical transistor can be summarized as follows. Emanating from both source and drain electrodes, metal wave functions penetrate in an evanescent regime through the molecule owing to its nonzero HOMO-LUMO gap. The overlap between these two waves, supported by the molecule, determines the tunnel current intensity through the source-to-drain molecular channels. As the HOMO-LUMO gap is progressively closed, the degree of delocalization of these evanescent waves increases over the molecule. This closure comes from an intra-HOMO and LUMO manifold repulsion effect that turns out to vary exponentially with the amount of orbital mixing in these manifolds introduced by gentle compression of the C_{60} cage. This very efficient valve action results from the way the delocalization of the metal wave on the molecule is controlled. This is a transistor effect in which the valve action results in the control of the electron transfer resistance between source and drain by a third, independent electrode.

A simple model of this transistor effect is a tunnel barrier whose height is modulated independently of its width and where its bias voltage remains much lower than the barrier height for the entire range of the electromechanical grid in working operation. The barrier-height modulation has been introduced by intentionally working in a tunnel transport regime supported by the C_{60} molecule. Such a modulation is difficult to obtain in a ballistic transport regime where there is no tunnel barrier, only a channel quantification effect which varies in an incremental noncontinuous manner. One solution to restore a barrier-height variation is to rely on a Schottky effect at the metal-molecule interface. In this case, the molecule must be sufficiently long with a very dense molecular level manifold near the Fermi level of the electrodes so that a Schottky barrier builds up. This was recently observed for a single carbon nanotube used as a ballistic molecular channel. A field-effect transistor was measured with a 100-nm-long nanotube. Such a length is required to stabilize the band-bending phenomenon.[35] The fundamental size limitation of such a device is the same as that for ultimate field-effect transistors: the channel must be sufficiently long ($L > 20$ nm) to ensure a good barrier formation at both ends.[36] In contrast, a one-order-of-magnitude shorter channel length can be obtained by working in a tunnel transport regime using the native tunnel barrier.

The price for this size reduction is the low intensity of the working tunnel current. Offsetting this is the benefit of a very short transit time of the electrons in the tunneling regime compared to the ballistic case. Working in the tunneling regime also opens up new avenues in terms of integrating more than one device per molecule. Our actual molecular electromechanical amplifier[1,2] and transistor[33] are discrete devices that may be associated in series or in parallel with an appropriate planar technology. But even more exciting is the possibility of integrating multiple devices in a single molecule. This requires that each subdevice be gated along a single molecule rather than electromechanically (or even electrically). In this sense, a ''current intensity'' gate seems better adapted for integrated molecular circuits if such a phenomenon can be mastered and developed at the nanoscale.

ACKNOWLEDGMENTS

This work was partially supported by the European Union ESPRIT MEL-ARI project ''Nanowires.'' The authors thank C. Coudret and A. Gourdon for chemical support, H. Pinna for electronic support, C. Bergaud for ''cantilever'' support, M. Magoga for complementary calculations, and P. Guéret and M. Welland for useful discussions.

[1] C. Joachim and J. K. Gimzewski, Chem. Phys. Lett. **265**, 353 (1997).
[2] C. Joachim and J. K. Gimzewski, Proc. IEEE **84**, 184 (1998).
[3] J. Bardeen and W. H. Brattain, Phys. Rev. **75**, 1208 (1949).
[4] M. A. McCord, A. Dans and R. F. N. Pease, J. Microelectromech. Syst. (to be published).
[5] G. Binnig and H. Rohrer, IBM J. Res. Dev. **30**, 355 (1986).
[6] J. K. Gimzewski and R. Möller, Phys. Rev. B **36**, 1284 (1987).
[7] D. P. E. Smith, Science **269**, 371 (1995).
[8] D. M. Eigler, C. P. Lutz, and W. E. Rudge, Nature (London) **352**, 600 (1991).
[9] C. Joachim, J. K. Gimzewski, R. R. Schlittler, and C. Chavy, Phys. Rev. Lett. **74**, 2102 (1995).
[10] U. Dürig, O. Züger, B. Michel, L. Häussling, and H. Ringsdorf, Phys. Rev. B **48**, 1711 (1993).
[11] V. Langlais, R. R. Schlittler, H. Tang, A. Gourdon, C. Joachim, and J. K. Gimzewski, Nature (London) (to be published).
[12] M. Magoga and C. Joachim, Phys. Rev. B **56**, 4722 (1997).
[13] N. D. Lang, IBM J. Res. Dev. **30**, 374 (1986).
[14] A. D. Stone and A. Szafer, IBM J. Res. Dev. **32**, 385 (1988).
[15] M. Büttiker, Y. Imry, R. Landauer, and S. Pinhas, Phys. Rev. B **31**, 6207 (1985).
[16] J. G. Simmons, J. Appl. Phys. **34**, 1793 (1963).
[17] C. Joachim and J. K. Gimzewski, Europhys. Lett. **30**, 409 (1995).
[18] R. Landauer and Th. Martin, Rev. Mod. Phys. **66**, 217 (1994).
[19] J. P. Spiller, T. D. Clark, R. J. Prance, and H. Prance, Europhys. Lett. **12**, 1 (1990).
[20] P. Sautet and C. Joachim, Phys. Rev. B **38**, 12 238 (1988).
[21] D. Lamoen, P. Ballone, and M. Parrinello, Phys. Rev. B **54**, 5097 (1996).
[22] P. Sautet and C. Joachim, J. Phys. C **21**, 3939 (1988).
[23] C. Joachim, J. P. Launay, and S. Woitellier, Chem. Phys. Lett. **147**, 131 (1990).
[24] P. Lainé, V. Marvaud, A. Gourdon, J. P. Launay, R. Azgazzi, and C. A. Bignozzi, Inorg. Chem. **35**, 711 (1996).
[25] C. Patoux, C. Coudret, J. P. Launay, C. Joachim, and A. Gourdon, Inorg. Chem. **36**, 5037 (1997).
[26] V. Marvaud, J. P. Launay, and J. Joachim, Chem. Phys. Lett. **177**, 23 (1993).
[27] P. Sautet and C. Joachim, Chem. Phys. Lett. **185**, 23 (1991)
[28] A. de Meijere and B. König, Synlett., 1221 (1997).
[29] S. Kammermeier, P. G. Jones, and R. Herges, Int. Ed. Engl. **35**, 2669 (1996).
[30] C. Joachim and J. K. Gimzewski, Probe Microsc. (to be published).
[31] See the special issue on electronics, IEEE Spectr. **17**, (1980).
[32] H. Tang, M. T. Cuberes, C. Joachim, and J. K. Gimzewski, Surf. Sci. **386**, 115 (1997).
[33] C. Joachim, C. Bergaud, H. Pinna, H. Tang, and J. K. Gimzewski, Ann. (N.Y.) Acad. Sci. (to be published).
[34] H. Tang, X. Bouju, C. Joachim, and C. Giraud, J. Chem. Phys. **108**, 359 (1998).
[35] S. J. Tano, A. R. W. Verschweren, and C. Dekker, Nature (London) **393**, 49 (1998).
[36] F. G. Pikus and K. K. Likharev, Appl. Phys. Lett. **71**, 3661 (1997).